Dating the termination of the Palaeoproterozoic Lomagundi-Jatuli carbon isotopic Event in the North Transfennoscandian Greenstone Belt

A. P. Martin[1*], D. J. Condon[1], A. R. Prave[2], V. A. Melezhik[3, 4], A. Lepland[3, 5], A. E. Fallick[6]

1 NERC Isotope Geosciences Laboratory, British Geological Survey, Keyworth, NG125GG, UK
2 Department of Earth Sciences, University of St Andrews, St Andrews, Scotland, UK
3 Geological Survey of Norway, Postboks 6315 Slupen, 7491 Trondheim, Norway
4 Centre for Geobiology, University of Bergen, Postboks 7803, N-5020 Bergen, Norway
5 Tallinn Technical University, Institute of Geology, 19086 Tallinn, Estonia
6 Scottish Universities Environmental Research Centre, East Kilbride, Glasgow G75 0QF, Scotland.
*adam@bgs.ac.uk

Abstract

Existing radio-isotopic age constraints indicate that the global Palaeoproterozoic Lomagundi-Jatuli large, positive carbonate carbon isotopic excursion, with $\delta^{13}C$ values > +5‰, occurred between 2.2 and 2.06 Ga. In the North Transfennoscandian Greenstone Belt of the Kola Peninsula, NW Russia, northern Norway and Finland, the Lomagundi-Jatuli Event is recorded in the carbonate rocks of the Umba and Kuetsjärvi Sedimentary formations in the Imandra-Varzuga and Pechenga greenstone belts. In both areas, thick mafic volcanic units (Umba and Kuetsjärvi Volcanic formations) overlie the sedimentary units recording the excursion. Overlying younger sedimentary units contain carbonate rocks with $\delta^{13}C$ values typically ranging between c. -1 and +3‰, signalling the termination of the Lomagundi-Jatuli excursion.

Two new U-Pb ID-TIMS (isotope-dilution thermal ionisation mass spectrometry) zircon dates constrain this termination in both successions. The lower unit of the Il'mozero Sedimentary Formation is a cross- and parallel-bedded volcaniclastic greywacke derived largely from erosion of the underlying Umba Volcanic Formation. It has yielded detrital zircons with $^{207}Pb/^{206}Pb$ dates as young as 2055.5 ± 2.3 Ma, which is a maximum age for deposition and is inferred to date part of the underlying Umba volcanics. In Pechenga, the Kolosjoki Sedimentary Formation was intersected by a drill hole obtained by the ICDP (International Continental Scientific Drilling Program) - supported FAR-DEEP (Fennoscandian Arctic Russia - Drilling Early Earth Project) drilling programme. Zircons from a mafic fine tuff in this drill core have yielded a $^{207}Pb/^{206}Pb$ age of 2056.6 ± 0.8 Ma. This age is interpreted as an eruption age contemporaneous with sedimentation. The new age determinations overlap each other within uncertainty, and is within error of previously published detrital zircon ages of 2058 ± 2 Ma from the Kolosjoki Sedimentary Formation and 2049 ± 28 Ma from the Kuetsjärvi Volcanic Formation. Combined, these indicate that the Lomagundi-Jatuli excursion terminated across Fennoscandia by 2056.6 ± 0.8 Ma and may correlate with similar termination ages in Fennoscandia and the Transvaal, South Africa.

Keywords: Lomagundi-Jatuli Event; U-Pb geochronology; Fennoscandia; Pechenga; Imandra-Varzuga; Palaeoproterozoic

1. Introduction

The early Proterozoic records Earth's transformation from an anoxic to an oxygenated planet and is characterised by intervals of global rifting, termination of major banded iron formation, appearance of red beds, and perturbations in the cycles and accumulation of sulphur, phosphate, and carbon. Among these perturbations, one of the largest known positive carbonate carbon isotope excursions, termed the Lomagundi-Jatuli Event (Melezhik et al., 2005), is unique in Earth history. During the Lomagundi-Jatuli Event $\delta^{13}C$ values of +10-15‰ V-PDB (Vienna Pee Dee Belemnite; all $\delta^{13}C$ values are relative to V-PDB hereafter) were not uncommon. Values of $\delta^{13}C$ of 0 ± 5‰ in marine carbonate rocks are typical throughout geological time (Shields and Veizer, 2002) and are considered to reflect a balance between organic and inorganic carbon pools at a ratio of approximately 1:4 (the Ronov ratio; Aharon, 2005). Positive excursions away from these *normal* near zero values are interpreted as either due to increased organic carbon productivity and burial, or reduced carbonate deposition. Thus carbon isotope excursions are proxies for large-scale transformations in the carbon cycle, possibly related to varying atmospheric-oceanic conditions, tectonic regimes, and biospheric evolution.

The origin of the name for the Lomagundi-Jatuli Event comes from the eponymous regions in Zimbabwe and Fennoscandia where strongly positive $\delta^{13}C$ values in Proterozoic carbonate rocks were first reported (Galimov et al., 1968; Schidlowski et al., 1975, 1976). Baker and Fallick (1989) suggested this excursion was global in nature and it has now been recognised on all continents except Antarctica. Karhu (1993), based on data from Fennoscandia, and Karhu and Holland (1996), who compiled all of the then existing radiometric ages, proposed that the Lomagundi-Jatuli Event occurred between 2.22 and 2.06 Ga. However, radiometric dates that can constrain tightly the initiation, duration, or termination of the excursion are few (see Melezhik et al., 2012b, for a recent review).

Here, we report two new, high precision U-Pb ID-TIMS (isotope dilution thermal ionisation mass spectrometry) zircon radiometric dates determined on samples obtained by a recent

ICDP (International Continental Scientific Drilling Program) -sponsored project, FAR-DEEP (Fennoscandian Arctic Russia - Drilling Early Earth Project; see http://www.icdp-online.org for details) in the Russian sector of Fennoscandia. These provide the first age constraint on the Lomagundi-Jatuli Event in the Imandra-Varzuga belt and further constrain its timing in Pechenga.

2. Geological Setting

Palaeoproterozoic supracrustal units in northern Fennoscandia crop out discontinuously over ~1000 km across the Kola Peninsula of NW Russia and from there into northern Norway and Finland (Fig. 1). They rest unconformably on Archaean rocks and are preserved in segments known as the Ust'ponoy, Imandra-Varzuga, Pechenga, Pasvik, Opukasjärvi, and Polmak Greenstone Belts (Fig. 1; Melezhik and Sturt, 1994). Collectively, these are termed the North Transfennoscandian Greenstone Belt. The best studied segment is Pechenga (Fig. 2), which hosts world-class nickel-sulphide deposits (Alapieti and Lahtinen, 2002), and is the site of the Kola Superdeep Drill Hole (Kozlovsky, 1987). The most aerially extensive segment is Imandra-Varzuga (Fig. 3), which extends for more than 350 km along strike. Sedimentary successions in both regions were the focus of FAR-DEEP, which recovered fresh diamond drill cores as well as samples from outcrop (Melezhik et al., 2012a).

2.1 Pechenga

The Pechenga supracrustal succession sits unconformably on Archaean basement and comprises the North and South Pechenga Groups. The former is composed of several alternating thinner sedimentary (1500 m total), and thicker volcanic formations (6500 m total; Melezhik and Sturt, 1994). The basal unit is the Neverskrukk Formation, consisting of polymict conglomerates and immature sandstones containing clastic material derived from the underlying basement complex (Fig. 2, 4). Above this are the mafic to intermediate lava flows and intrusive rocks of the Amahlati Formation that, in turn, are overlain by the Kuetsjärvi Sedimentary Formation. It is in this latter unit, consisting of red-coloured sandstone and carbonate rocks, including stromatolitic carbonates, that the Lomagundi-Jatuli excursion is recorded, with $\delta^{13}C$ values $\leq +9‰$ (Melezhik et al., 2007). The sedimentary units are overlain by mafic to felsic alkaline volcanic rocks with subordinate volcaniclastic conglomerates of the Kuetsjärvi Volcanic Formation. In sharp contact on those igneous rocks is the Kolosjoki Sedimentary Formation, marked by basal volcaniclastic and arkosic sandstones and then a succession of finer sandstones, dolomitic carbonates and minor tuffs; the carbonate rocks have $\delta^{13}C$ values mostly between $+1 \leq \delta^{13}C$ ‰ $\leq +2.5$ (Melezhik et al., 2007). The overlying Kolosjoki Volcanic Formation is tholeiitic basalts and mafic tuffs with subordinate ferropicritic extrusive rocks and is overlain by the Pilgujärvi Sedimentary Formation. The latter consists of carbonaceous- and sulfide-rich turbidite sandstones, fine-grained siliciclastic rocks, and minor, mafic and ferropicritic tuffs and lavas at the top of the formation. The Pilgujärvi Sedimentary Formation also contains several economic, ultramafic-hosted, sulphide, Ni-Cu deposits. The topmost unit of the North Pechenga Group is the Pilgujärvi Volcanic Formation consisting of pillowed and massive tholeiitic lava flows and subordinate ferro-picrite flows and felsic tuffs. More detailed descriptions of Pechenga geology are in Melezhik and Sturt (1994), Sharkov and Smolkin (1997), and references therein.

2.2 Imandra-Varzuga

The lowermost rocks of the Imandra-Varzuga supracrustal succession are tholeiitic basalts and polymict sandstones of the Purnach Formation and overlying Kuksha Sedimentary (arkosic sandstone, greywacke, conglomerate) and Volcanic (tholeiitic basalt) formations that sit unconformably on Archaean basement (Fig. 3, 4). The succeeding Seidorechka Sedimentary Formation consists mostly of flaser-bedded greywacke-shale, cross-bedded and rippled quartzitic sandstones, parallel-bedded siltstones and a thin dolostone that has $\delta^{13}C$ values between -1.8 and +3.5‰ (Melezhik and Fallick, 1996). These rocks are overlain by komatiitic-basaltic lava flows and tuffs of the Seidorechka Volcanic Formation and by the inferred Huronian-equivalent glacial deposits of the Polisarka Sedimentary Formation, with siltstone and sandstone beds including dropstones and polymict conglomerates. The glacial rocks are then overlain by spinifex-textured lava flows, volcanic breccias, and intermediate lava flows that comprise the Polisarka Volcanic Formation. The Umba sedimentary-volcanic couplet occurs above those lavas and consists of red-coloured, cross-bedded sandstones, siltstones, and dolostones overlain by mafic and intermediate alkaline lava flows and subordinate picrites. The Umba dolostones are interpreted as recording the Lomagundi-Jatuli excursion with $\delta^{13}C$ values $\leq +6.7$‰ (Melezhik and Fallick, 1996). Resting erosionally on the Umba volcanic rocks is the Il'mozero Sedimentary Formation, which consists of cross- and parallel-bedded volcaniclastic greywacke and siltstones, black shales, dolostones, and stromatolitic dolostones having $\delta^{13}C$ values from -0.8 to +2.4‰ (Melezhik and Fallick, 1996). Tholeiitic lava flows, tuffs, and lava breccias of the Il'mozero Volcanic Formation overlie these sedimentary units. See Melezhik and Sturt (1994) and Sharkov and Smolkin (1997) for further geological descriptions.

2.3 *Existing Chronology*

In Pechenga, the Archaean basement is cross-cut by the General'skaya gabbro-norite intrusion dated by $^{207}Pb/^{206}Pb$ ID-TIMS (zircon) at 2505 ± 1.6 Ma (Amelin et al., 1995), providing a maximum age for the supracrustal rocks (Fig. 4). The middle part of the Kuetsjärvi Volcanic Formation and the base of the Kolosjoki Sedimentary Formation consist of volcaniclastic conglomerates and greywackes sourced from the Kuetsjärvi Volcanic Formation, from which detrital zircons have been recovered and dated by $^{207}Pb/^{206}Pb$ ID-TIMS at 2058 ± 2 Ma (Melezhik et al., 2007), and as such provides a maximum age for the stratigraphic level sampled within the Kolosjoki Sedimentary Formation. Melezhik et al. (2007) argued for the underlying volcanic rocks being the only probable source of the youngest detrital zircons in the Kolosjoki Sedimentary Formation and thus infer a c. 2058 Ma age for part of the Kuetsjärvi Volcanic Formation (Fig. 4). A minimum age has been determined on detrital zircons in the Kuetsjärvi Volcanic Formation at 2049 ± 28 Ma in volcaniclastic conglomerates which crop out with an erosional contact on the irregular palaeosurface of alkaline felsic lava breccias in the middle of the formation (Melezhik et al., 2007; Fig. 4). A felsic volcanic unit in the Pilgujärvi Volcanic Formation (Fig. 4) has yielded an ID-TIMS $^{207}Pb/^{206}Pb$ zircon age at 1970 ± 5 Ma (Hanski et al., 1990). The lower Kuksha Volcanic Formation in Imandra-Varzuga is intruded by the Monche Pluton and the Pana Tundra Intrusion, dated by U-Pb ID-TIMS (zircon) at 2504.4 ± 1.5 and 2501.5 ± 1.7 Ma (Amelin et al., 1995), providing a minimum age constraint for the Kuksha Volcanic Formation (Fig. 4). Magmatic bodies interpreted as feeder dykes and intrusions related to the Seidorechka Volcanic Formation yield $^{207}Pb/^{206}Pb$ dates of 2442.2 ± 1.7 Ma (baddeleyite) on a sub-volcanic unit and 2441 ± 1.6 Ma (zircon) on the spatially associated Imandra lopolith (both by U-Pb ID-TIMS; Amelin et al., 1995; Fig. 4).

3. Sample Descriptions

In order to better constrain the timing of the Lomagundi-Jatuli excursion, the Il'mozero Sedimentary Formation in Imandra-Varzuga, and the Kolosjoki Sedimentary Formation in Pechenga, were sampled for U-Pb dating. Sample Il'mozero 1 was collected from outcrop (67°06'45.0" N, 035°41'23.5" E; Fig. 3) in the lowermost Il'mozero Sedimentary Formation. It yielded zircons that were analysed by laser ablation inductively coupled plasma mass spectrometry (LA-ICPMS) and by ID-TIMS. Sample 8B 151.42m is from the Kolosjoki Sedimentary Formation and was obtained from diamond drill core of Hole 8B of FAR-DEEP in the Pechenga belt. It yielded zircons that were dated by the ID-TIMS method.

3.1 Sample Il'mozero 1 (Imandra-Varzuga)

In outcrop the Il'mozero Sedimentary Formation sits unconformably on the Umba Volcanic Formation (Fig. 2, 4). Sample Il'mozero 1 is part of an interbedded succession of thin-bedded sandstone and shale that occurs approximately 50 m above the contact with the underlying Umba lava flows; the rocks are at lower greenschist facies. In hand specimen, it is a fine-grained greywacke that exhibits grading and cm-scale layering. Cleavage is well-developed and at a high angle to bedding. The middle part of the Il'mozero Sedimentary Formation (c. 30-40 m above the stratigraphic horizon of sample Il'mozero 1) is marked by 10 m of interbedded shale and light grey dolostones that record normal $\delta^{13}C$ values (Melezhik and Fallick, 1996). In thin section bedding is defined by a change in grain size from c. 80 µm to 50 µm, with well-sorted, poorly rounded grains (Fig. 5a; S1a). Quartz is the most common mineral: pyroxene and plagioclase are minor at 1-2 volume percent (visual estimation; Fig. S1b, c). The pyroxene is euhedral and acicular, ≤ 300 µm long, with 87^{o} cleavage, is pleochroic on the [100] face (α) from green to green-yellow and displays second-order birefringence, optical properties that are consistent with augite. These primary grains are overprinted by chlorite and pyrite. Augite and plagioclase are key mafic rock minerals that break-down quickly in the sedimentary environment; their presence suggests a proximal, (ultra-) mafic igneous source, presumably the underlying Umba Volcanic Formation. The morphology of the zircons recovered from sample Il'mozero 1 was variable between elongated, clear grains ≤ 200 µm in size with medial melt inclusion traces and sub-rounded, equant grains ≤ 100 µm in size (Fig. S2). Cathode luminescence images show growth zoning typical of magmatic crystals, with rare rims on the equant grains (Fig. S2).

3.2 Sample 8B 151.42m (Pechenga)

Sample 8B 151.42m is derived from the 336 m long FAR-DEEP drillcore 8B (69^{o}27'56''N, 30^{o}32'08'' E; Fig. 2) that intersects the Kolosjoki Sedimentary Formation. The base of the Kolosjoki Sedimentary Formation occurs at c. 322 m in the drill core where the first sandstone bed that sits on rocks inferred to be intermediate volcanic lava flows and tuffs. Above this, the remaining 322 m consist mostly of sandstone units with minor greywacke and carbonate layers. The core interval 90 to 190 m is characterised by elevated chromium and nickel concentrations and is interpreted to be composed largely of ultramafic tuffs (Melezhik et al., 2012c).

In hand specimen, fragments of crystals and scoria (c. 500 μm) have a common alignment, giving the rock a discontinuous, streaky appearance (Fig. 5b). The sampled unit is 6 cm thick, melanocratic, and exhibits a sharp upper and lower contact in hand specimen. In thin section the lower contact (the upper contact is not visible in the thin section) is sharp; below the contact scoria and crystal fragments (500 μm) are absent (Fig. S1d). There is a bi-modal size distribution (Fig. S1e, f), with larger (500 μm) scoria clasts and plagioclase crystals supported by finer-grained crystals (20 μm). Many of the plagioclase crystals have been pseudomorphed by pyrite. There is also extensive carbonate alteration (Fig. S1e) from the breakdown of volcanic glass. Scoria clasts are elongate, with rough and ragged edges, and a near uniform size of 500 μm on the long axis (Fig. S1f). The fragments and crystals are not commonly found as epiclasts (Boggs, 2010; Pettijohn et al., 1987), and given their rough edges and common angularity (Fig. S1e, f), indicate little or no re-working, consistent with the absence of sedimentary features. These characteristics suggest that sample 8B 151.42m is a primary igneous deposit, with the scoria and larger crystals part of a porphyritic texture in a fine-grained groundmass. The preservation of plagioclase, and the melanocratic colour index indicate a mafic composition and the rock is best interpreted as a mafic fine tuff (classification after White and Houghton, 2006), subsequently altered to lower greenschist facies. Zircon crystals (20 – 70 μm; Fig. S2) were extracted from a 6-cm-long (1/4 core) sample between 151.42 m and 151.48 m in FAR-DEEP drill core 8B.

4. Methods

Zircons were analysed using a combined LA-ICPMS and ID-TIMS methodology at the NERC Isotope Geoscience Laboratory (NIGL), Keyworth, U.K. The LA-ICPMS method yields radiometric dates on the detrital zircon population in sample Il'mozero 1, and provide a means to identify suitable chronology targets prior to dissolution for ID-TIMS analysis. All zircons were subject to a modified chemical abrasion pre-treatment for the elimination of Pb-loss (Mattinson, 2005). The $^{207}Pb/^{206}Pb$ dates are based upon the dual decay of ^{238}U to ^{206}Pb and ^{235}U to ^{207}Pb, and their accuracy is controlled by the precision and accuracy of the radiogenic $^{207}Pb/^{206}Pb$ ratio, the present-day $^{238}U/^{235}U$ ratio, and the decay constants of ^{235}U and ^{238}U (see section 4.1 and online supplemental material for details and further discussion). In order to obviate any issues related to non-zero age Pb-loss and compromised $^{207}Pb/^{206}Pb$ dates we place an emphasis on zircon U-Pb data that are concordant at the high-level of precision afforded by the ID-TIMS method. For carbonate stable isotope analysis, 1 mg samples were dissolved overnight in phosphoric acid at 70^{o} C. Isotope ratios were measured at the Scottish Universities Environment Research Council on PRISM III and AP2003 mass spectrometers. Repeat analyses of NBS-18 and internal calcite standards are generally better than ± 0.2‰.

4.1 *Comment on dating methods and uncertainties*

In this contribution published radio-isotopic dates are combined with new data and this requires consideration of systematic uncertainties associated with these dates. Firstly, when comparing dates derived from different isotopic decay schemes the systematic uncertainty related to the decay constant value must be considered (see Condon and Bowring, 2011, for a recent review). However, when assessing the relative ages of samples dated using the same decay scheme, it is sufficient to consider only uncertainty derived from non-systematic sources. Secondly, recent studies have suggested that the natural $^{238}U/^{235}U$ ratio should no longer be considered invariant and is not equal to 137.88 (Condon et al., 2010; Hiess et al., 2012; Stirling et al., 2007), and a value of 137.818 ± 0.045 has been suggested for use in U-Pb zircon geochronology (Hiess et al., 2012). Using this more accurate value with its associated uncertainty has the effect of lowering $^{207}Pb/^{206}Pb$ dates at c. 2 Ga by 0.8 ± 0.6 Myr. In this study, $^{207}Pb/^{206}Pb$ dates cited have been determined using a $^{238}U/^{235}U$ value equal to 137.88. In Table S1 (online summary table) we list the interpreted dates for the samples of interest calculated using both $^{238}U/^{235}U$ = 137.88 and 137.818 ± 0.045.

5. Results

5.1 U-Pb

5.1.1 Sample Il'mozero 1

LA-ICPMS: Results less than 5% discordant are included on a relative probability plot of $^{207}Pb/^{206}Pb$ ages from LA-ICPMS data in Fig. S3. Over 50% of the $^{207}Pb/^{206}Pb$ ages are between 2100 and 2000 Ma, with a concentration of ages between c. 2080 and 2060 Ma (Table 1). The youngest $^{207}Pb/^{206}Pb$ age in this range is 2063 ± 9 Ma (1.4% discordant). Grains in the age range 2080 to 2060 Ma have magmatic growth zoning and equant morphology (Fig. S2) and grains with this morphology were subsequently targeted for ID-TIMS analysis.

ID-TIMS: Seven single zircon crystals were analysed by ID-TIMS (Table 2). One grain (z1) is slightly discordant (Fig. 6a), indicating minor Pb-loss. The $^{207}Pb/^{206}Pb$ dates for the six other grains (z2, z4 - 6, z9, z12) overlap within uncertainty (Fig. 6b), with z9 yielding the youngest $^{207}Pb/^{206}Pb$ date at 2055.5 ± 2.3 Ma. A second grain (z12) yielding a $^{207}Pb/^{206}Pb$ date of 2055.67 ± 2.3 Ma, gives confidence that youngest zircon (z9) has not experienced any minor Pb-loss and is an appropriate youngest age. Incorporation of the uncertainties in $\lambda^{235}U$ and $\lambda^{238}U$ (Jaffey et al., 1971) increases the uncertainty to 2.4 Myr. The ages yielded from the youngest zircon grains by ID-TIMS and LA-ICPMS overlap within uncertainty. Based upon the concordant U-Pb systematics and the morphology of the dated zircons, the $^{207}Pb/^{206}Pb$ date of 2055.5 ± 2.3/2.4 Ma (analytical/total uncertainty) is interpreted to reflect the maximum age of sample Il'mozero 1 and therefore the Il'mozero Sedimentary Formation at this stratigraphic level.

5.1.2 Sample 8B 151.42m

ID-TIMS: Seven single zircon crystals were analysed by ID-TIMS (Table 2) yielding concordant data (Fig. 6a) and $^{207}Pb/^{206}Pb$ dates between 2053.7 ± 4.7 and 2057.6 ± 2.3 Ma, which overlap within uncertainty (Fig. 6b) and yield an error weighted mean $^{207}Pb/^{206}Pb$ date of 2056.6 ± 0.8 Ma (n = 7, MSWD = 0.89); this implies that the seven zircons are equivalent in age. Incorporation of the uncertainties in $\lambda^{235}U$ and $\lambda^{238}U$ (Jaffey et al., 1971) increases the uncertainty to 0.9 Myr. Based upon the concordant U-Pb systematic and the morphology of the dated zircons the $^{207}Pb/^{206}Pb$ date of 2056.6 ± 0.8/0.9 Ma (analytical/total uncertainty) is interpreted to reflect the age of the mafic fine tuff and the age of the sampled stratigraphic level.

5.2 Stable isotopes

Carbon and oxygen isotope data measured on carbonate samples from the Il’mozero Sedimentary Formation are shown in Table 3. The $\delta^{13}C$ values range from a minimum of -0.7‰ to a maximum of +2.6‰ and the $\delta^{18}O$ values vary between -13.8 and -9.3‰ (relative to Vienna Standard Mean Ocean Water: V-SMOW). The carbonate samples overlie by c. 10 m the dated sample Il’mozero 1.

6. Discussion

The 2055.5 ± 2.3 Ma age obtained from detrital zircons in the Il’mozero Sedimentary Formation is the first robust age from the upper part of the Imandra-Varzuga succession. The proximity of carbonates with normal $\delta^{13}C$ values above the dated interval, and the underlying $\delta^{13}C$ values up to +6.7‰, indicate that 2055.5 ± 2.3 Ma constrains the tail end, or termination, of the Lomagundi-Jatuli Event in this part of the North Transfennoscandian Greenstone Belt. The 2055.5 ± 2.3 Ma age from Imandra-Varzuga is a maximum age for the Il’mozero Sedimentary Formation at this stratigraphic level. However, based upon the stratigraphic relationship of the dated Il’mozero 1 sample overlying the Umba Volcanic Formation, and petrography, it is inferred that the 2055.5 ± 2.3 Ma also dates part of the Umba Volcanic Formation volcanic rocks and approximates the timing of sediment accumulation/volcanism at this broad stratigraphic level. A similar argument is presented in Melezhik et al. (2007), where zircon dated at 2058 ± 2 Ma in volcaniclastic-rich sediments in the Kolosjoki Sedimentary Formation, Pechenga, is interpreted to date the underlying Kuetsjärvi Volcanic Formation.

The dated tuff horizon in FAR-DEEP drill hole 8B from the Kolosjoki Sedimentary Formation is interpreted as an eruption age, syn-depositional with sedimentation, and thus the 2056.6 ± 0.8 Ma age directly constrains the age at this stratigraphic level. Rocks immediately under and overlying sample 8B 151.42m record normal $\delta^{13}C$ values (Fig. S4) and overlie the Kuetsjärvi Sedimentary Formation (separated by the Kuetsjärvi Volcanic Formation; Fig. 4) that bears the Lomagundi-Jatuli anomalous carbon isotope signature. The obtained age, therefore, dates the termination of the Lomagundi-Jatuli Event. This date overlaps, within uncertainty, with the c. 2055 to 2060 Ma detrital zircon dates (Il’mozero and Kolosjoki Sedimentary Formation; Fig. 6b, c) that are inferred to closely approximate the timing of broadly contemporaneous (Umba) volcanism. The Kolosjoki Sedimentary and Il’mozero

Sedimentary formations have long been considered as litho- and chemo-stratigraphic equivalents (e.g. Melezhik and Sturt, 1994). The new age data confirm that they are also chronostratigraphic equivalents, strengthening correlations between the two units. The new carbon isotope data (Table 3) are consistent with existing data from the Il'mozero Sedimentary Formation showing $\delta^{13}C$ values between -0.8 and +2.4‰ (Melezhik and Fallick, 1996) and signal a return to normal $\delta^{13}C$ values following the Lomagundi-Jatuli Event.

In Fennoscandia, the duration of the Lomagundi-Jatuli Event was first defined as 2200 – 2060 Ma (Karhu, 1993) and a termination age of 2050 ± 8 Ma (zircon; ID-TIMS) was inferred based on felsic volcanic rocks associated with carbonate rocks having normal $\delta^{13}C$ values at the top of the Peräphoja Belt on the Karelia craton (Perttunen and Vaasjoki, 2001). This overlaps, within uncertainty, with the 2056.6 ± 0.8 Ma age on the North Transfennoscandian Greenstone Belt on the Kola craton. Initially, the Lomagundi-Jatuli Event was thought to have continued at least until 2078 ± 8 Ma on Fennoscandia, based upon ID-TIMS data from titanite and zircon fractions on an intrusive sill in the Kuusamo Schist Belt (zircon and titanite fractions; ID-TIMS; Silvennoinen, 1991). Utilising this constraint, the termination of the Lomagundi-Jatuli Event on Fennoscandia could be constrained to between 2078 ± 8 and 2056.6 ± 0.8 Ma. However, the primary nature of the dated titanite fractions that provide this constraint have recently been called into question (Hanski et al., 2001). If this is accepted, then the next closest age constraints are c. 2200 Ma (e.g. Perttunen, 1991; Perttunen & Vaasjoki 2001; Silvennoinen, 1991).

Units recording the Lomagundi-Jatuli Event crop out in the Silverton Formation of the Transvaal Supergroup in South Africa, with $\delta^{13}C$ values between +2 and +10‰ (Frauenstein et al., 2009). Stratigraphically overlying the Silverton Formation, carbonate rocks in the Houtenbek Formation record a return to normal $\delta^{13}C$ values between -3.3 and -0.5‰ (Melezhik and Fallick, 2010, and references therein). Above this formation (and separated by the Dullstroom lava), the intrusions of the Bushveld Complex yield zircons dated by the U-Pb ID-TIMS technique at 2054 ± 2 Ma (Scoates and Friedman, 2008), providing a minimum age for the termination of the Lomagundi-Jatuli Event in the Transvaal Basin. Thus, age constraints for the termination of the Lomagundi-Jatuli Event overlap, within uncertainty, between Fennoscandia (2056.6 ± 0.8 Ma, North Transfennoscandian Greenstone Belt; 2050 ±

8 Ma, Peräphoja Schist Belt) and South Africa (2054 ± 2 Ma, Transvaal Basin). The focussing of radio-isotopic age constraints on the transition from positive to normal $\delta^{13}C$ values at c. 2060 Ma is also suggestive of global synchronism.

7. Conclusions

The two largest and economically important segments of the North Transfennoscandian Greenstone Belt in NW Russia (Pechenga and Imandra-Varzuga) can be correlated based upon litho-, chemo-, and now chrono-stratigraphy, with radiometric ages at 2056.6 ± 0.8 Ma (Kolosjoki Sedimentary Formation) and 2055.5 ± 2.3 Ma (Il'mozero Sedimentary Formation). This complements the existing radiometric ages of 2058 ± 2 Ma and 2049 ± 28 Ma (Melezhik et al., 2007) from Pechenga. The termination of the Lomagundi-Jatuli Event in the North Transfennoscandian Greenstone Belt, and Fennoscandia, can be confined to > 2056.6 ± 0.8 Ma. This overlaps with, within error, the termination of the Lomagundi-Jatuli Event from the Transvaal Supergroup, South Africa, constrained at > 2054 ± 2 Ma (Scoates and Friedman, 2008).

Acknowledgements

APM, DJC, and ARP are supported by NERC grant NE/G00398X/1. VAM is supported by NFR grant 191530/V30 (projects 331000 and 802795).

References

Aharon, P., 2005. Redox stratification and anoxia of the early Precambrian oceans: Implications for carbon isotope excursions and oxidation events. Precambrian Research 137, 207-222.

Alapieti, T.T., Lahtinen, J.J., 2002. Platinum-Group Element Mineralization in Layered Intrusions of Northern Finland and the Kola Peninsula, Russia, in: Cabri, L.J. (Ed.), The Geology, Geochemistry, Mineralogy and Mineral Benefication of Platinum-group Elements. CIM Special Volume 54, pp. 507-546.

Amelin, Y.V., Heaman, L.M., Semenov, V.S., 1995. U-Pb geochronology of layered mafic intrusions in the eastern Baltic Shield: implications for the timing and duration of Paleoproterozoic continental rifting. Precambrian Research 75, 31-46.

Baker, A.J., Fallick, A.E., 1989. Evidence from Lewisian limestones for isotopically heavy carbon in two-thousand-million-year old sea water. Nature 337, 352-354.

Boggs, S.J., 2010. Petrology of Sedimentary Rocks, 2nd ed. Cambridge University Press, Cambridge.

Condon, D.J., Bowring, S.A., 2011. Chapter 9 A user's guide to Neoproterozoic geochronology. Geological Society, London, Memoirs 36, 135-149.

Condon, D.J., McClean, N., Noble, S.R., Bowring, S.A., 2010. Isotopic composition ($^{238}U/^{235}U$) of some commonly used uranium reference materials. Geochimica et Cosmochimica Acta 74, 7127-7143.

Frauenstein, F., Veizer, J., Beukes, N., Van Niekerk, H.S., Coetzee, L.L., 2009. Transvaal Supergroup carbonates: Implications for Palaeoproterozoic $\delta^{18}O$ and $\delta^{13}C$ records. Precambrian Research 175, 149-160.

Galimov, I.M., Kuznetsova, N.G., Prokhorov, V.S., 1968. The problem of the composition of the Earth's ancient atmosphere in connection with results of isotopic analyses of carbon from Precambrian carbonates. Geochemistry 11, 1376-1381 (in Russian).

Hanski, E.J., Huhma, H., Smol'kin, V.F., Vaasjoki, M., 1990. The age of ferropicritic volcanites and comagmatic Ni-bearing intrusions at Pechenga, Kola Peninsula, U.S.S.R. Geological Survey of Finland Bulletin 62, 123-133.

Hanski, E.J., Huhma, H., Vaasjoki, M., 2001. Geochronology of northern Finland: A summary and discussion. Geological Survey of Finland, Special Paper 33, 255-279.

Hiess, J., Condon, D.J., McClean, N., Noble, S.R., 2012. $^{238}U/^{235}U$ systematics in terrestrial U-bearing minerals. Science 335, 1610-1614.

Jaffey, A.H., Flynn, K.F., Glendenin, L.E., Bentley, W.C., Essling, A.M., 1971. Precision measurement of half-lives and specific activities of ^{235}U and ^{238}U. Physics Reviews, C4, 1889-1906.

Karhu, J.A., 1993. Palaeoproterozoic evolution of the carbon isotope ratios of sedimentary carbonates in the Fennoscandian Shield. Geological Survey of Finland Bulletin 371, 1-87.

Karhu, J.A., Holland, H.D., 1996. Carbon isotopes and the rise of atmospheric oxygen. Geology 24, 867-870.

Kozlovsky, Y.A., 1987. The Superdeep Well of the Kola Peninsula. Spinger Verlag, Berlin, p. 558.

Mattinson, J.M., 2005. Zircon U-Pb chemical abrasion ("CA-TIMS") method: Combined annealing and multi-step partial dissolution analysis for improved precision and accuracy of zircon ages. Chemical Geology 220, 47-66.

Melezhik, V., Prave, A., Fallick, A., Hanski, E., Lepland, A., Kump, L., Strauss, H., 2012a. Reading the Archive of Earth's Oxygenation. Springer, Heidelberg (in press).

Melezhik, V.A., Fallick, A.E., 1996. A widespread positive $\delta^{13}C$ carb anomaly at around 2.33-2.06 Ga on the Fennoscandian Shield: a paradox? Terra Nova 8, 141-157.

Melezhik, V.A., Fallick, A.E., 2010. On the Lomagundi-Jatuli carbon isotopic event: The evidence from the Kalix Greenstone Belt, Sweden. Precambrian Research 179, 165-190.

Melezhik, V.A., Fallick, A.E., Hanski, E., Kump, L., Lepland, A., Prave, A., Strauss, H., 2005. Emergence of the aerobic biosphere during the Archean-Proterozoic transition: Challenges for future research. Geological Society of America Today 15, 4-11.

Melezhik, V.A., Fallick, A.E., Martin, A.P., Condon, D.J., Kump, L.R., Brasier, A.T., Salminen, P., 2012b. The greatest perturbation of the global carbon cycle: the Lomagundi-Jatuli isotopic event, in: Melezhik, V., Prave, A., Fallick, A., Hanski, E., Lepland, A., Kump, L., Strauss, H. (Eds.), Reading the Archive of Earth's Oxygenation. Volume 2: The Core Archive of the Fennoscandian Arctic Russia-Drilling Early Earth Project. Springer, Heidelberg (in press).

Melezhik, V.A., Huhma, H., Condon, D.J., Fallick, A.E., Whitehouse, M.J., 2007. Temporal constraints on the Paleoproterozoic Lomagundi-Jatuli carbon isotopic event. Geology 35, 655-658.

Melezhik, V.A., Prave, A.R., Lepland, A., Hanski, E.J., Romashkin, A.E., Rychanchik, D.V., Luo, Z.-Y., 2012c. Kuetsjärvi Sedimentary Formation: FAR-DEEP Hole 5A, neighbouring quarry and related outcrops, in: Melezhik, V., Prave, A., Fallick, A., Hanski, E., Lepland, A., Kump, L., Strauss, H. (Eds.), Reading the Archive of Earth's Oxygenation. Volume 2: The Core Archive of the Fennoscandian Arctic Russia-Drilling Early Earth Project. Springer, Heidelberg (in press).

Melezhik, V.A., Sturt, B.A., 1994. General geology and evolutionary history of the early Proterozoic Polmak-Pasvik-Pechenga-Imandra/Varzuga-Ust'Ponoy Greenstone Belt in the northeastern Baltic Shield. Earth-Science Reviews 36, 181-204.

Perttunen, V., Vaasjoki, M., 2001. U-Pb geochronology of the Perapohja schist belt, northwestern Finland. Special Paper Geological Survey of Finland 33, 45-84.

Pettijohn, F.J., Potter, P.E., Siever, R., 1987. Sand and Sandstone, 2nd ed. Springer-Verlag, New York.

Schidlowski, M., Eichmann, R., Junge, C.E., 1975. Precambrian sedimentary carbonates: carbon and oxygen isotope geochemistry and implications for the terrestrial oxygen budget. Precambrian Research 2, 1-69.

Schidlowski, M., Eichmann, R., Junge, C.E., 1976. Carbon isotope geochemistry of the Precambrian Lomagundi carbonate province, Rhodesia. Geochimica et Cosmochimica Acta 40, 449-455.

Scoates, J.S., Friedman, R.M., 2008. Precise age of the platiniferous Merensky Reef, Bushveld Complex, South Africa, by the U-Pb zircon chemical abrasion ID-TIMS technique. Economic Geology and the Bulletin of the Society of Economic Geologists 103, 465-471.

Sharkov, E.V., Smolkin, V.F., 1997. The early Proterozoic Pechenga-Varzuga Belt: a case of Precambrian back-arc spreading. Precambrian Research 82, 133-151.

Shields, G.A., Veizer, J., 2002. The Precambrian marine carbonate isotope database: version 1.1. Geochemistry, Geophysics, Geosystems 3, 10.1029/2001GC000266.

Silvennoinen, A., 1991. Kuusamon ja Rukatunturin kartta-alueiden kallioperä. Summary: Pre-Quaternary rocks of the Kuusamo and Rukatunturi map-sheet areas. Explanation to the maps of Pre-Quaternary rocks, sheets 4524+4542. Geological map of Finland 1:100,000, 63 p.

Stirling, C.H., Andersen, M.B., Potter, E.K., Halliday, A.N., 2007. Low-temperature isotopic fractionation of uranium. Earth and Planetary Science Letters 264, 208-225.

White, J.D.L., Houghton, B.F., 2006. Primary Volcaniclastic Rocks. Geology 34, 677-680.

Figure 1. Location of the segments of the North Transfennoscandian Greenstone Belt.

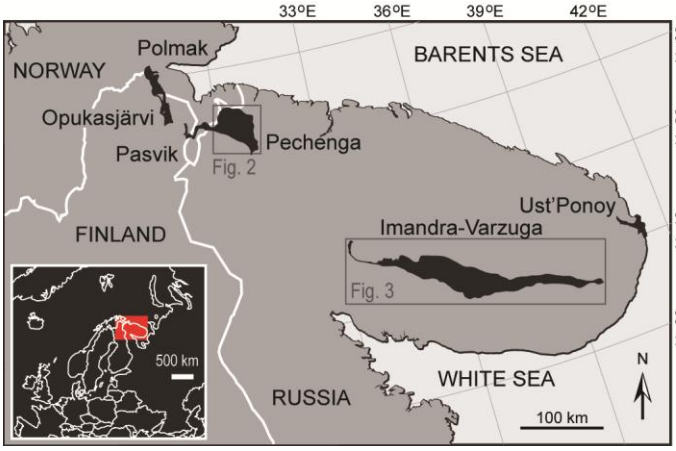

Figure. 2. The Pechenga Greenstone Belt after Melezhik and Sturt (1994). See the text for a description of the units and Fig. 4 for the stratigraphic column.

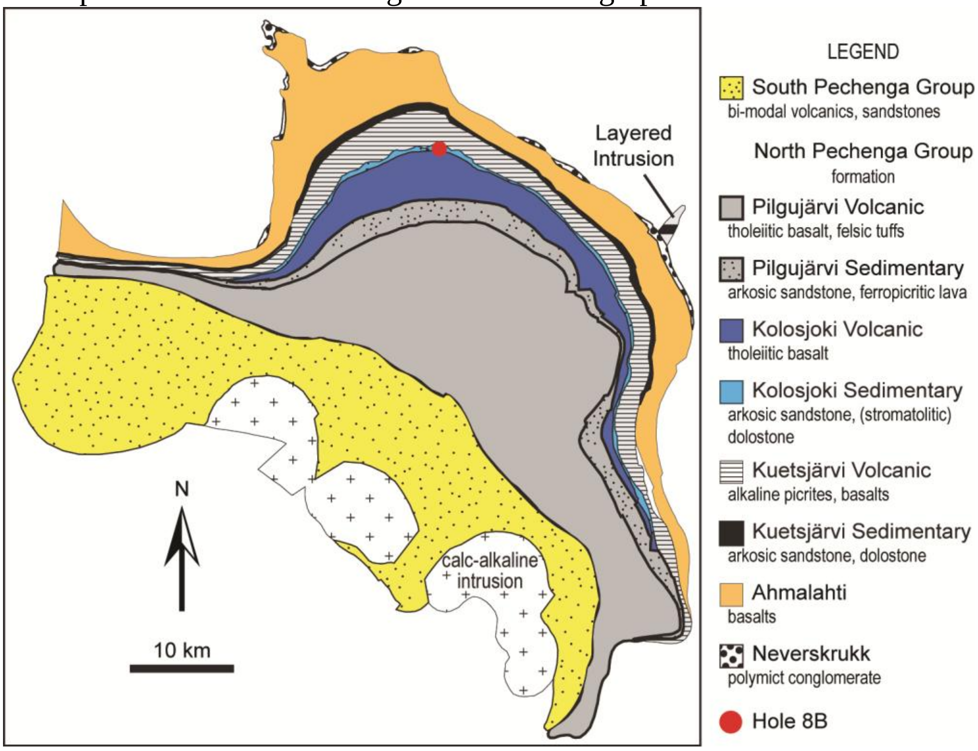

Figure 3. The Imandra-Varzuga Greenstone Belt after Melezhik and Sturt (1994). See the text for a description of the units and Fig. 4 for the stratigraphic column.

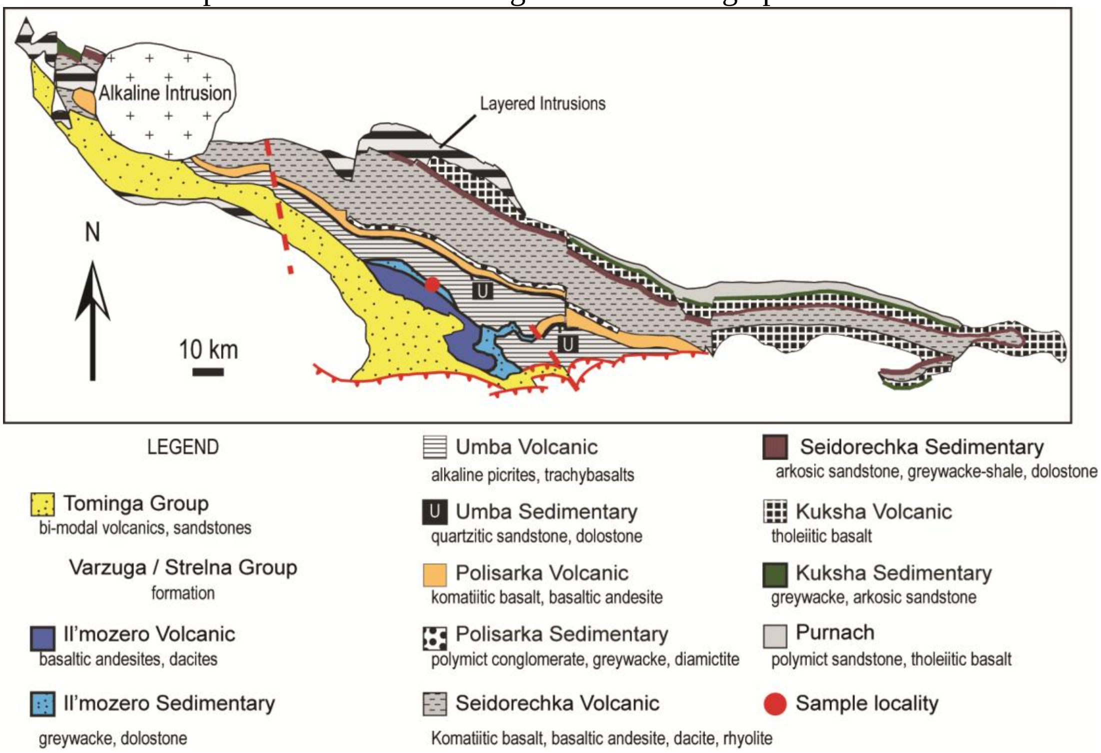

Figure. 4. Stratigraphic columns after Melezhik and Sturt (1994) of a. The Pechenga Greenstone Belt, and b. The Imandra-Varzuga Greenstone Belt. The new radiometric dates (this study) are boxed. Published, relevant ages are from: 1. Hanski et al. (1990); 2. Melezhik et al. (2007); 3. Amelin et al. (1995). R = rhyolite (granite); D = dacite (granodiorite); A = andesite (diorite); B = basalt (gabbro); P = picrite (ultramafic). The patterns used for formations in the stratigraphic columns match those used for formations in Fig. 2 and 3. The values in the Group column are maximum reported $\delta^{13}C$ values (‰ V-PDB) for the adjacent formation, taken from: A: (Melezhik et al., 2007); B. (Melezhik and Fallick, 1996Melezhik and Fallick, 1996).

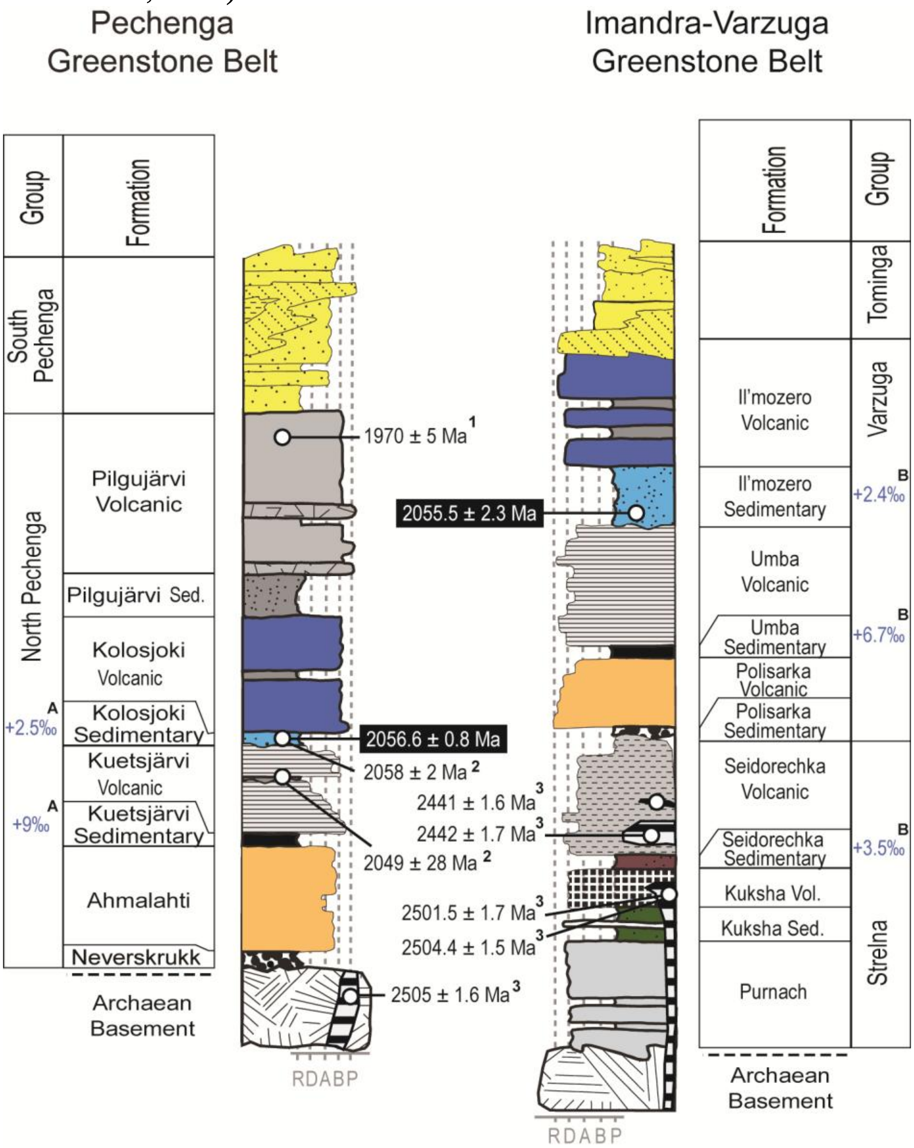

Figure 5. Petrography of dated samples. a. Il’mozero 1 in thin section. b. A scanned image of Sample 8B 151.42m in hand specimen. Fragments of pumice, crystals (feldspar), and rare jasper are visible.

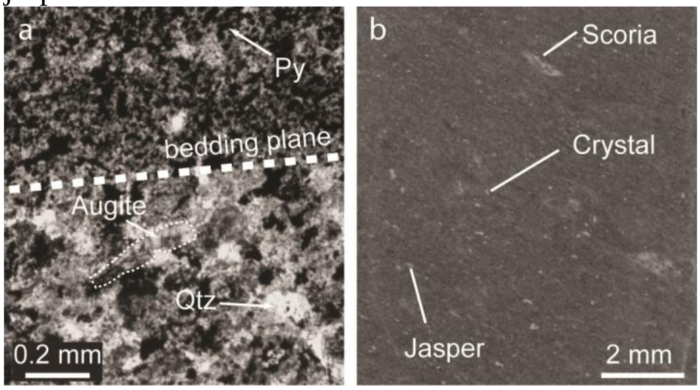

Figure 6. a. Conventional concordia plot for zircons from samples Il'mozero 1 (Imandra-Varzuga) and 8B 151.42m (Pechenga) for single zircon grains analysed by the ID-TIMS method. The data from Melezhik et al. (2007) from single zircon grains from the Kolosjoki Sedimentary Formation (from Pechenga and the same formation as sample 8B 151.42m) are included for comparison. b. ^{207}Pb-^{206}Pb plot of data from Fig. 6a.

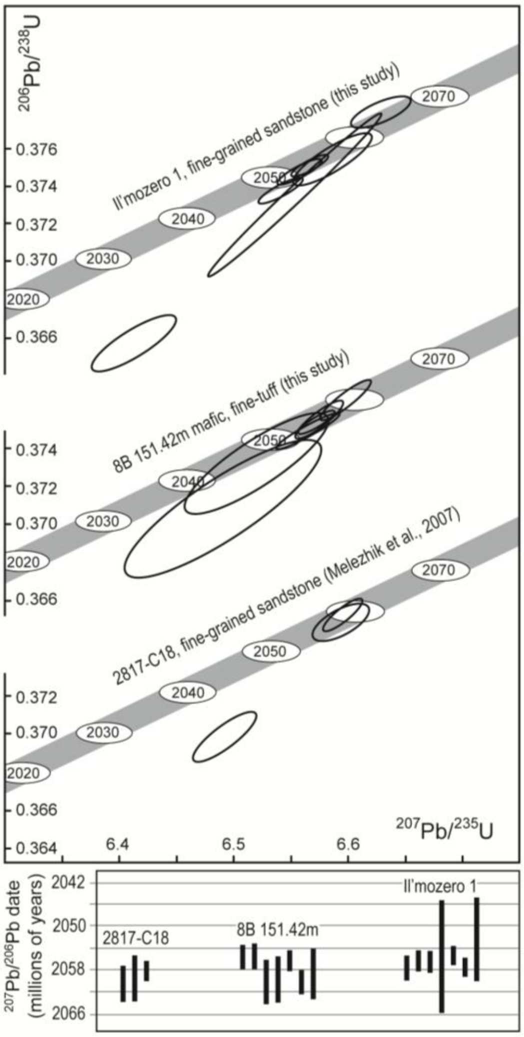

Table 1 Zircon U-Pb LA-ICPMS data for sample Il’mozero 1.

Zr	Signals						Ratios									Isotopic ages						
	^{204}Pb (cps)	^{206}Pb (mV)	^{207}Pb (mV)	^{238}U (mV)	Pb (ppm)	U (ppm)	^{238}U/^{206}Pb	1σ %	^{207}Pb/^{206}Pb	1σ %	^{207}Pb/^{235}U	1σ %	^{206}Pb/^{238}U	1σ %	Rho	^{207}Pb/^{206}Pb	2σ abs	^{206}Pb/^{238}U	2σ abs	^{207}Pb/^{235}U	2σ abs	% conc.
1	18	3.0	0.7	8.2	74	124	1.71	1.01	0.2405	0.50	19.3866	1.13	0.5846	1.01	0.90	3123.4	8.0	2967.4	48.1	3061.3	21.6	95.0
3	231	2.6	0.5	8.0	63	121	1.93	1.21	0.1984	1.10	14.1409	1.64	0.5169	1.21	0.74	2813.2	17.9	2686.0	53.2	2759.2	30.6	95.5
6	126	5.8	1.0	17.7	142	269	1.96	1.36	0.1948	0.50	13.6830	1.45	0.5094	1.36	0.94	2783.4	8.2	2653.9	58.9	2728.0	27.1	95.3
10	-227	10.9	1.3	46.3	265	704	2.73	1.26	0.1284	0.50	6.4800	1.36	0.3659	1.26	0.93	2076.6	8.8	2010.2	43.4	2043.2	23.6	96.8
14	187	4.4	1.0	11.3	106	172	1.64	0.88	0.2426	0.50	20.3781	1.01	0.6093	0.88	0.87	3136.8	7.9	3067.3	42.6	3109.5	19.3	97.8
15	71	3.0	0.4	12.9	73	196	2.74	0.93	0.1290	0.50	6.4957	1.05	0.3651	0.93	0.88	2084.9	8.8	2006.3	31.9	2045.3	18.4	96.2
17	142	10.8	1.3	46.5	264	707	2.72	0.90	0.1301	0.50	6.5944	1.03	0.3677	0.90	0.87	2098.9	8.8	2018.6	31.1	2058.6	18.0	96.2
18	-90	3.7	0.4	15.5	90	236	2.66	0.96	0.1284	0.50	6.6677	1.08	0.3766	0.96	0.89	2076.3	8.8	2060.4	33.8	2068.3	19.0	99.2
19	-70	2.1	0.5	5.0	51	76	1.52	0.97	0.2750	0.50	24.9618	1.09	0.6584	0.97	0.89	3334.6	7.8	3260.9	49.6	3306.7	21.1	97.8
20	101	8.1	1.4	24.3	197	370	1.90	1.35	0.1880	0.50	13.6164	1.44	0.5252	1.35	0.94	2725.2	8.2	2721.0	59.6	2723.4	26.8	99.8
21	139	11.6	1.4	49.0	283	746	2.69	1.01	0.1294	0.50	6.6366	1.13	0.3719	1.01	0.90	2090.3	8.8	2038.2	35.3	2064.2	19.7	97.5
22	65	12.3	1.4	50.6	300	770	2.67	1.13	0.1280	0.50	6.6054	1.24	0.3743	1.13	0.91	2070.3	8.8	2049.8	39.6	2060.1	21.6	99.0
23	-69	7.2	0.8	30.5	174	464	2.72	0.94	0.1277	0.50	6.4748	1.06	0.3677	0.94	0.88	2066.9	8.8	2018.4	32.5	2042.5	18.6	97.7
24	45	7.0	1.0	24.4	170	371	2.22	0.98	0.1606	0.50	9.9750	1.10	0.4505	0.98	0.89	2461.7	8.4	2397.7	39.3	2432.5	20.2	97.4
26	-36	3.0	0.4	13.0	74	197	2.73	1.03	0.1295	0.52	6.5444	1.16	0.3666	1.03	0.89	2090.7	9.2	2013.5	35.7	2051.9	20.2	96.3
27	153	5.6	0.6	23.7	135	360	2.72	0.94	0.1276	0.50	6.4708	1.06	0.3678	0.94	0.88	2065.1	8.8	2019.1	32.5	2041.9	18.6	97.8
28	310	2.0	0.2	8.5	48	130	2.77	1.01	0.1292	0.50	6.4351	1.12	0.3613	1.01	0.90	2086.7	8.8	1988.5	34.4	2037.1	19.6	95.3
29	241	21.2	6.7	45.5	516	692	1.36	0.94	0.3469	0.50	35.0611	1.07	0.7331	0.94	0.88	3693.4	7.6	3544.8	51.1	3640.4	20.8	96.0
30	184	13.8	1.6	58.5	337	890	2.74	1.07	0.1279	0.50	6.4380	1.18	0.3649	1.07	0.91	2069.9	8.8	2005.5	36.8	2037.5	20.6	96.9
31	126	11.7	2.8	28.5	285	433	1.57	1.01	0.2606	0.50	22.9629	1.13	0.6390	1.01	0.90	3250.6	7.9	3185.0	50.5	3225.4	21.7	98.0
32	79	5.7	0.7	24.1	139	366	2.70	0.92	0.1274	0.50	6.5192	1.05	0.3710	0.92	0.88	2063.0	8.8	2034.1	32.2	2048.5	18.3	98.6
33	613	21.5	2.6	90.5	523	1377	2.67	1.01	0.1341	1.29	6.9126	1.63	0.3739	1.01	0.62	2152.2	22.4	2047.6	35.3	2100.3	28.6	95.1
34	69	5.4	0.6	23.6	132	359	2.76	1.11	0.1280	0.50	6.3964	1.22	0.3623	1.11	0.91	2071.1	8.8	1993.2	38.0	2031.8	21.2	96.2
35	-186	9.1	1.7	25.9	221	395	1.82	0.91	0.2090	0.50	15.8551	1.04	0.5503	0.91	0.88	2897.6	8.1	2826.3	41.5	2868.1	19.6	97.5
36	-233	5.0	0.8	16.4	121	249	2.09	0.95	0.1766	0.50	11.6675	1.08	0.4792	0.95	0.89	2621.2	8.3	2523.6	39.7	2578.1	19.9	96.3
37	189	10.3	1.2	43.3	251	659	2.58	2.01	0.1345	0.98	7.1840	2.24	0.3874	2.01	0.90	2157.6	17.2	2110.6	72.1	2134.5	39.2	97.8

40	-54	4.7	0.5	21.2	116	323	2.85	0.90	0.1233	0.50	5.9554	1.03	0.3504	0.90	0.87	2003.8	8.9	1936.7	29.9	1969.4	17.7	96.6
41	-102	6.5	0.8	27.0	158	411	2.65	0.86	0.1320	0.50	6.8715	1.00	0.3775	0.86	0.87	2124.9	8.8	2064.6	30.4	2095.0	17.5	97.2
46	-247	7.9	0.9	33.4	192	509	2.71	0.97	0.1279	0.50	6.5066	1.09	0.3688	0.97	0.89	2069.9	8.8	2023.9	33.5	2046.8	19.0	97.8
47	-239	8.4	1.0	35.8	204	544	2.68	1.08	0.1297	0.50	6.6694	1.19	0.3728	1.08	0.91	2094.6	8.8	2042.6	37.6	2068.6	20.8	97.5
51	-56	9.7	1.7	29.7	238	452	1.94	1.01	0.1925	0.50	13.6591	1.13	0.5145	1.01	0.90	2764.0	8.2	2675.8	44.1	2726.4	21.1	96.8
52	-73	1.0	0.2	2.8	24	43	1.79	0.88	0.2205	0.59	16.9648	1.06	0.5579	0.88	0.83	2984.5	9.5	2858.1	40.6	2932.8	20.2	95.8
58	34	7.6	0.9	32.8	185	499	2.73	1.03	0.1299	0.50	6.5547	1.15	0.3660	1.03	0.90	2096.5	8.8	2010.5	35.6	2053.3	20.0	95.9
59	130	19.1	2.3	81.9	464	1246	2.72	0.86	0.1297	0.50	6.5727	0.99	0.3675	0.86	0.86	2094.1	8.8	2017.6	29.6	2055.7	17.3	96.3
60	-66	13.5	1.6	57.5	328	875	2.71	0.90	0.1283	0.50	6.5309	1.03	0.3692	0.90	0.87	2074.8	8.8	2025.6	31.2	2050.1	18.0	97.6

Table 2 U-Th-Pb data for zircons analysed by ID-TIMS from samples Il'mozero 1. and 8B 151.42m.

Fraction							Radiogenic Isotope Ratios								Isotopic Ages					
	Th/U	$^{206}Pb^*$ $\times 10^{-13}$ mol	mol % $^{206}Pb^*$	Pb^*/Pb_c	Pb_c (pg)	$^{206}Pb/^{204}Pb$	$^{208}Pb/^{206}Pb$	$^{207}Pb/^{206}Pb$	% err	$^{207}Pb/^{235}U$	% err	$^{206}Pb/^{238}U$	% err	corr. coef.	$^{207}Pb/^{206}Pb$	±	$^{207}Pb/^{235}U$	±	$^{206}Pb/^{238}U$	±
(a)	(b)	(c)	(c)	(c)	(c)	(d)	(e)	(e)	(f)	(e)	(f)	(e)	(f)		(g)	(f)	(g)	(f)	(g)	(f)
Il'mozero 1.																				
z1	0.786	1.1112	96.92%	11	2.92	592	0.229	0.127137	0.268	6.409819	0.472	0.365655	0.328	0.834	2058.70	4.74	2033.62	4.15	2008.98	5.66
z2	0.721	1.6171	98.88%	29	1.52	1627	0.208	0.127245	0.128	6.552413	0.955	0.373474	0.936	0.991	2060.19	2.25	2052.97	8.41	2045.79	16.41
z4	0.890	2.2009	99.17%	41	1.52	2196	0.256	0.126964	0.107	6.565059	0.208	0.375021	0.123	0.915	2056.30	1.89	2054.67	1.83	2053.04	2.17
z5	0.556	3.9797	93.30%	4	24.04	263	0.160	0.127131	0.404	6.568396	0.754	0.374718	0.539	0.856	2058.62	7.13	2055.12	6.64	2051.63	9.47
z6	0.668	1.0618	97.09%	11	2.64	625	0.192	0.127246	0.232	6.585170	0.428	0.375338	0.297	0.856	2060.21	4.10	2057.36	3.78	2054.53	5.22
z9	0.661	2.5597	99.05%	34	2.03	1924	0.190	0.126907	0.131	6.555718	0.228	0.374656	0.136	0.860	2055.50	2.31	2053.41	2.01	2051.33	2.39
z12	0.416	2.0918	98.66%	23	2.36	1354	0.120	0.126920	0.130	6.539981	0.248	0.373720	0.155	0.892	2055.67	2.30	2051.30	2.18	2046.95	2.72
8B 151.42m																				
z7	1.102	0.7030	94.99%	6	3.30	313	0.316	0.126777	0.268	6.578309	0.388	0.376335	0.230	0.737	2053.70	4.74	2056.45	3.42	2059.19	4.05
z10	0.579	1.1636	99.42%	55	0.56	3154	0.166	0.127051	0.102	6.574262	0.207	0.375290	0.132	0.913	2057.51	1.79	2055.90	1.82	2054.31	2.32
z11	0.578	1.3082	99.37%	51	0.69	2890	0.166	0.126899	0.101	6.554642	0.223	0.374620	0.155	0.918	2055.38	1.78	2053.27	1.96	2051.17	2.73
z12	0.524	0.5316	93.06%	4	3.53	225	0.151	0.127043	0.322	6.575673	0.469	0.375394	0.289	0.738	2057.39	5.68	2056.09	4.14	2054.80	5.08
z20	0.721	1.5560	99.04%	33	1.30	1739	0.207	0.126989	0.103	6.575766	0.208	0.375560	0.128	0.921	2056.64	1.81	2056.10	1.83	2055.57	2.26
z21	0.548	0.7336	99.25%	43	0.46	2439	0.157	0.126969	0.109	6.575673	0.244	0.375614	0.177	0.914	2056.36	1.92	2056.09	2.15	2055.83	3.12
z24	0.469	0.5306	98.79%	26	0.54	1498	0.135	0.127062	0.129	6.596177	0.290	0.376510	0.218	0.908	2057.64	2.28	2058.84	2.56	2060.03	3.85

(a) z1, z2 etc. are labels for fractions composed of single zircon grains or fragments; all fractions annealed and chemically abraded after Mattinson (2005).

(b) Model Th/U ratio calculated from radiogenic $^{208}Pb/^{206}Pb$ ratio and $^{207}Pb/^{235}U$ age.

(c) Pb^* and Pb_c represent radiogenic and common Pb, respectively; mol % $^{206}Pb^*$ with respect to radiogenic, blank and initial common Pb.

(d) Measured ratio corrected for spike and fractionation only.

(e) Corrected for fractionation, spike, and common Pb; up to 1 pg of common Pb was assumed to be procedural blank: $^{206}Pb/^{204}Pb = 18.20 \pm 0.50\%$; $^{207}Pb/^{204}Pb = 15.65 \pm 0.40\%$; $^{208}Pb/^{204}Pb = 38.20 \pm 0.75\%$ (all uncertainties 1-sigma). Excess over blank was assigned to initial common Pb.

(f) Errors are 2-sigma, propagated using the algorithms of Schmitz and Schoene (2007).

(g) Calculations are based on the decay constants of Jaffey et al. (1971). $^{206}Pb/^{238}U$ and $^{207}Pb/^{206}Pb$ ages corrected for initial disequilibrium in $^{230}Th/^{238}U$ using Th/U [magma] = 4. $^{206}Pb/^{238}U$ dates in bold are those used in the weighted mean zircon date calculation

Table 3. The $\delta^{13}C$ and $\delta^{18}O$ values from carbonate rocks in the Il'mozero Sedimentary Formation (‰ relative to Vienna Pee Dee Belemnite and Standard Mean Ocean Water).

sample	height (m)	$\delta^{13}C$ ‰	$\delta^{18}O$ ‰
ILM-1	0.5	-0.7	-13.8
ILM-2	1.0	1.5	-13.3
ILM-3	2.5	2.0	-12.0
ILM-4	3.5	2.2	-11.7
ILM-5	5.5	2.6	-10.9
ILM-6	7.0	2.5	-10.6
ILM-7	9.0	2.5	-9.3

Height (m) = the height in metres above the contact between the greywacke and first carbonate rock in the Il'mozero Sedimentary Formation.